Use of an optical chronograph for deep investigation of natural water reservoirs

L.E. Arushanyan, V.G. Atanesyan, T.A. Gevorkyan, A.A. Nazaryan, A.A. Frangyan, and A.A. Tsovyan

Armyan-Greece Closed Company "Lazernaya Tekhnika–Pirkal," Erevan

Received July 24, 2002

A high-sensitive K-008 camera was used for taking images of test objects of various shapes and size located at different depths in water with various hydrooptical characteristics. Dependences of image contrast and signals reflected from an object on the depth of object location, its reflection coefficient, and angular size have been obtained. Satisfactory agreement with theoretical calculations was achieved. Field measurements were carried out in Lake Sevan.

Methods of laser remote sensing find wide-range applications to investigation of the World Ocean.[1,2] These methods are used to determine the primary hydrooptical characteristics (PHC) of seawater, to study their fine structure and the spatiotemporal variability. Introduction of an imaging channel in such systems (see, for example, Ref. 3) extends the range of such investigations. This is very important from the viewpoint of both basic research and applied problems, including ecological and geological ones and others.

When observing objects under water, one of the main characteristics is image contrast, whose increase is the main problem in vision at large depths. For this purpose, gating of the return signal is usually used.

The power of the reflected signal received at orientation of the observation system at the object's center is a sum of three components[4]:

$$P_I = P_{ob} + P_{bs}^{o} + P_{bs}^{e}, \quad (1)$$

where P_{ob} is the power of radiation reflected by the object's surface; P_{bs}^{o} is the power of backscattering noise from the depth of the medium in front of the object; P_{bs}^{e} is the power of backscattering noise from the depth of the medium behind the object (taking into account its screening effect).

When the observation system is oriented at the medium area beyond the object, the equation for the received power takes the form

$$P_{bs} = P_{bs}^{o} + P_{bs}^{\infty}, \quad (2)$$

where P_{bs}^{∞} is the power of backscattering noise from the depth of the medium located behind the object (without the object's screening effect).

The equation for determination of the object's image contrast against the background of the medium can be written as follows[4]:

$$K = (P_I - P_{bs})/(P_I + P_{bs}). \quad (3)$$

These equations allow us to analyze the behavior of the image contrast depending on the parameters of the object and the observation system, as well as the medium characteristics, just which was the aim of this study.

The experimental laser setup was capable of recording images of objects located at different depths. We have studied the dependence of the image contrast on the object's depth, its angular dimensions, the reflection coefficient of the object's surface, and water PHC.

The power of the output radiation of the second harmonic of a pulsed YAP:Nd laser varied within 0–200 mJ; the duration of the laser and gating pulses was ~ 12 ns; the angle of illumination varied from 10^{-3} to 0.5 rad; the viewing angle varied from 0.1 to 0.5 rad; the sensitivity was from 0 to 10^{-12} W; the exposure time was from 10^{-7} to 10^{-8} s; the linear scanning speed was 10^{-7}–10^{-9} s/cm. Images were recorded with a high-sensitivity K-008 electrooptic chronograph,[6] capable of recording and measuring the spatiotemporal parameters of fast processes in both single-frame mode and in the mode of linear scanning of the studied image. Image recording and processing were performed on a personal computer with the corresponding software.

In the process of investigations, we have conducted series of field and laboratory measurements.

Field measurements were conducted at Lake Sevan under the following experimental conditions: the angle of incidence onto the interface was roughly 67°, the distance from the observation system to the water surface was ~ 50 m, the maximum object's depth (along the beam path) was 13.5 m, the wavelength was 540 nm, the duration of the laser and gating pulses was ~ 12 ns, and the energy density was 10 mJ/m^2. The studied objects ~ 240 mm in diameter had a spherical or cylindrical shape (cylinder with the height of 700 mm). Water PHC were determined using a Secchi disc.[5]

Figure 1 shows characteristic frames recorded at Lake Sevan. Frame (*a*) was obtained in the linear scanning mode, when the angular size of the observation field is larger than the angular dimensions of the object. The object is

0235-6880/03/02 141-04 $02.00

a full sphere with the diameter of 240 mm and the reflection coefficient $R \sim 0.3$ located at the depth of 7 m. Frame (*c*) was obtained in the single-frame mode. This frame shows the cylindrically shaped object with the distributed reflection coefficient[5] at the depth of 4 m.

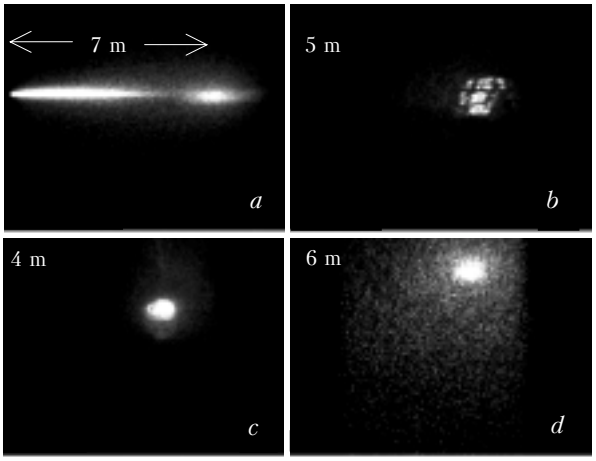

Fig. 1. Characteristic images of objects obtained in field investigations. Transparency by the Secchi disk is 6 m: (*a*) image of a full sphere 240 mm in diameter (reflection coefficient $R \sim 0.3$) located at the depth of 7 m, the image was obtained in the mode of linear scanning (scanning speed of 30 ns/cm). The diameter of the spot on the water surface ~ 100 mm. From left to right: the time the beam touches the medium interface – the left edge of the clearly seen elliptical figure; the clearly seen large ellipse – beam passage through the hydrosphere (the 7-m part of the path from the object's boundary); smaller ellipse is the object. The entire area exposed on the frame except for the object itself is the backscattering background area; (*b*) sphere image disturbed by waves – the image is fragmented and broken, the object's shape is distorted; (*c*) image of the cylindrical object with the base diameter of 240 mm and the height of 700 mm located at the depth of 4 m. The reflection coefficient of the end part ~ 0.3. The side surface of the object – equally thick stripes of white ($R \sim 0.3$) and black ($R \sim 0.01$) color; (*d*) image of the spherical object 240 mm in diameter obtained from the limiting visibility depth.

Frame (*b*) demonstrates how the image of a spherical object breaks[5] under the effect of the rough water surface: the image is fragmented and broken, and the object's shape is distorted. Frame (*d*) demonstrates the image of a spherical object obtained from the limiting visibility depth equal to 6 m according to the Secchi disc. The image is partly fragmented.[5]

The experimentally obtained dependence of the image contrast K for the full sphere 240 mm in diameter on the depth h in field investigations is depicted in Fig. 2 (the energy density on the water surface was roughly 10 mJ/m^2, the angular size of the observation field was larger than the object's angular dimensions, the object's reflection coefficient was $R \sim 0.3$).

One can see the characteristic decrease of the contrast, which satisfactorily agrees with the calculated curve.[4] The water extinction coefficient calculated by these data $\varepsilon \sim 0.56$ m^{-1} agrees well with that obtained from direct measurements by the Secchi disc.[5]

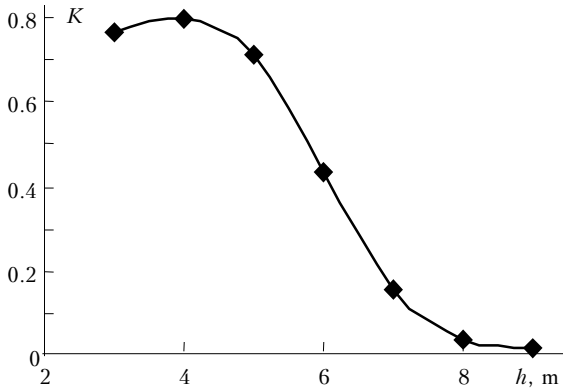

Fig. 2. Dependence of the image contrast K on the object's depth h (as the object we used a white full sphere 240 mm in diameter, with the reflection coefficient ~ 0.3; the transparency by the Secchi disc was ~ 6 m).

Figure 3*a* in the top row shows the images of spherical objects located at the depth of 4 m and having the same angular size of 5 mrad, but different surface reflection coefficients R, whose values are presented in Fig. 3*a*. The bottom row under the objects' images presents the images of their shadows from the depth of 7 m. In these frames we can see the effect of the reflection coefficient on the image contrast and the angular size of the shadow.

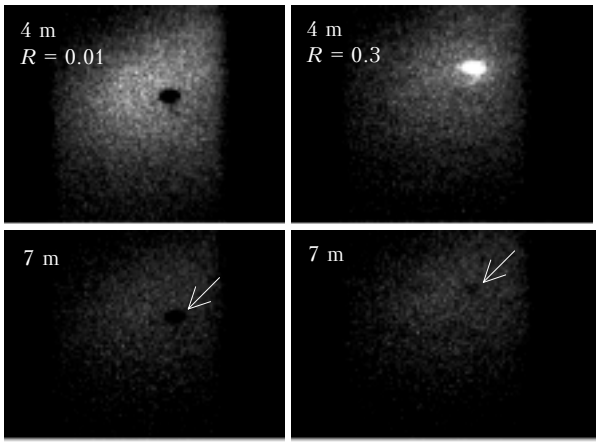

Fig. 3*a*. Images of objects with different reflection coefficients R and their shadows: top row – images of the black ($R \sim 0.01$) and white ($R \sim 0.3$) spheres 240 mm in diameter located at the depth of 4 m; bottom row – images of objects' shadows from the depth of 7 m.

The experimental dependence of the image contrast for the same objects and their shadows in the case of depth scanning is shown in Fig. 3*b*: at the depth of 2 m one can see that the leading edge of the beam touches the objects, at the depth of 4 m the contrast is the highest, and at the depth of 6 m the trailing edge of the beam touches the object (the beam falls under the object into the shadow area). In the plot we can clearly see different depth dependences of the shadow image contrast (starting from 6 m corresponding to the depth by the Secchi disk) for different reflection coefficients of the objects' surfaces, which was not earlier reported. In theoretical

calculations[4] the effect of the reflection coefficient was completely ignored.

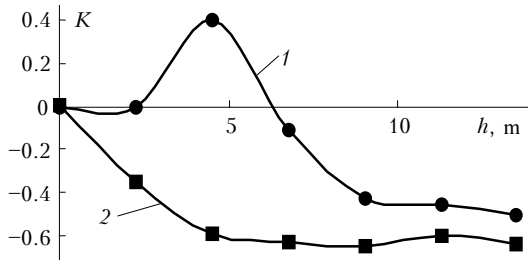

Fig. 3*b*. Depth dependence of the image contrast K for the object and its shadow: $K(h)$ for the white sphere 240 mm in diameter with the reflection coefficient ~ 0.3 and its shadow (curve *1*); $K(h)$ for the black sphere of the same size with the reflection coefficient ~ 0.01 and its shadow (curve *2*); transparency by the Secchi disc in the both cases ~ 6 m, the curves correspond to the object's shadow starting from the depth of 6 m.

Under laboratory conditions, a water body was modeled by a tube 33 m in length and 0.7 m in diameter, which was coated from inside with special paint having the reflection coefficient ~ 1% at the wavelength used, and therefore it could not serve as a secondary illumination source. Targets were modeled by plane (0.5 mm thick) rectangular objects of different dimensions (100 × 80, 280 × 115 mm, etc.) with the reflection coefficients from 0.02 to 0.5. The laser radiation wavelength was 540 nm, the duration of the laser and gating pulses was ~ 12 ns, the output energy density was 10 mJ/m^2, and the incidence of laser radiation onto the water surface was close to vertical. Water PHC for the laboratory setup were measured with a photometer. Images were recorded by the same method as in the field experiments.

Figure 4*a* shows the images of a rectangular object for different depth as recorded with the laboratory setup at the water transparency of 15 m by the Secchi disc. At the depth of 15 m the image was completely broken. Figures 4*b–d* depict the laboratory dependences of the image contrast on different parameters.

It can be seen from Fig. 4*b* that the image contrast for objects with different reflection coefficients grew with the depth. At the depth of 9 m, which makes up ~ 0.8 of the Secchi disc depth, it achieves the maximum value, and then the dependence has a drop-down character. This behavior of contrast is characteristic of objects with the reflection coefficient exceeding the effective reflection coefficient[4] of the gated medium layer. Figure 4*c* depicts the depth dependence of the image contrast for objects of different size. The size of the illuminated spot on the water surface was the same for all the objects, and the reflection coefficient was ~ 0.2. It can be seen that the contrast behavior in this case is the same, but the image contrast for small-size objects is always higher than that for large objects.

Figure 4*d* illustrates the depth dependence of the image contrast for objects of the same size with the same reflection coefficients, but for different values of the water extinction coefficient ε. It can be seen that as the medium extinction coefficient decreases, both the growth and drop-down rates of the contrast increase.

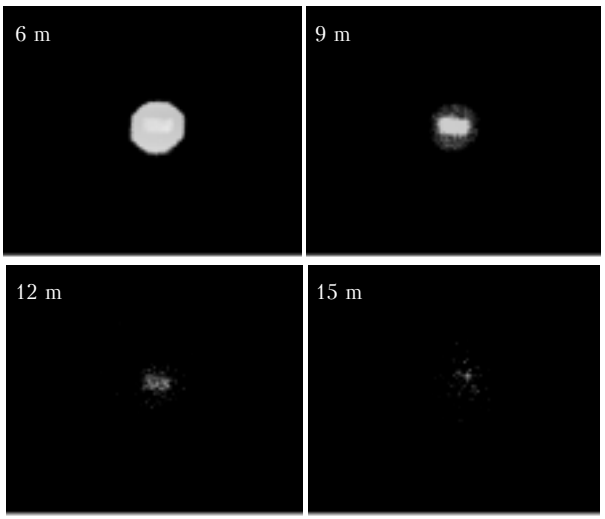

Fig. 4*a*. Images of a rectangular object obtained in the laboratory experiment from the depth of 6, 9, 12, and 15 m. Transparency of ~ 15 m by the Secchi disc.

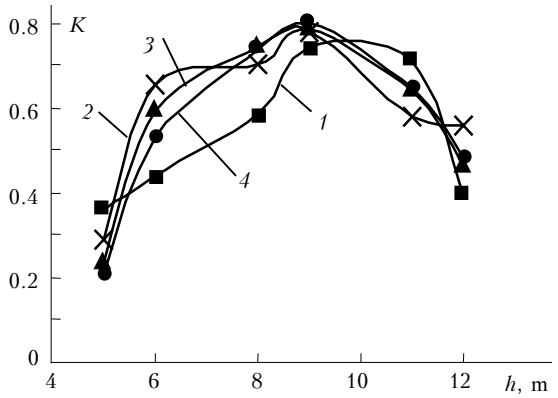

Fig. 4*b*. Depth dependence of the image contrast K for objects with different reflection coefficients R: ~ 0.02 (curve *1*), ~ 0.05 (*2*), ~ 0.2 (*3*), ~ 0.25 (*4*). The water transparency by the Secchi disc in this experiment was ~ 11 m, and the object dimensions were 100 × 80 mm.

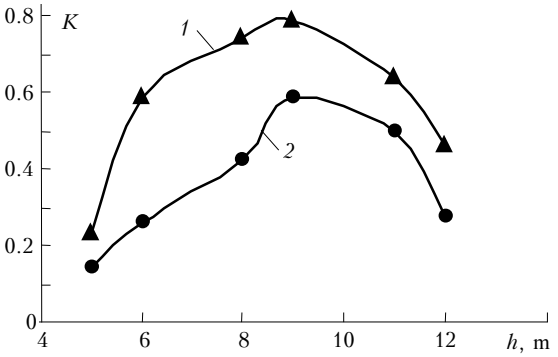

Fig. 4*c*. Depth dependence of the image contrast K for objects with different dimensions (the reflection coefficients for the both objects R ~ 0.20, water transparency by the Secchi disc ~ 11 m): 100 × 80 mm (curve *1*), 280 × 115 mm (*2*).

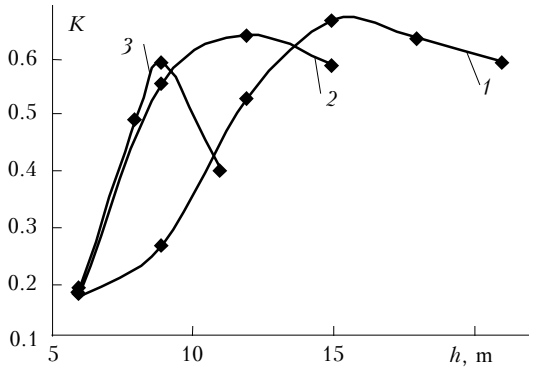

Fig. 4*d*. Depth dependence of the image contrast K for different values of the water extinction coefficient ε (the reflection coefficient of all the objects R ~ 0.2, the dimensions 280 × 115 mm): ε = 0.27 (curve *1*), 0.36 (*2*), 0.46 m^{-1} (*3*).

The peak of the image contrast is observed at the depth about 0.8 of the limiting visibility depth, but for objects of the same type at the limiting depth, the peak is possible for the medium with higher transparency.

Figures 5*a* and *b* depict the laboratory depth dependences of the reflection signal from an object S and the image background F in relative units for different values of the reflection coefficient of the object's surface (energy density on the water surface is roughly the same, about 10 mJ/m^2, the angular size of the observation field is larger than the angular size of an object, the water transparency by the Secchi disk is 11 m). In Fig. 5*a* we can see a monotonic behavior of the depth dependence of the signal (for different reflection coefficients of the objects).

Thus, based on the results obtained we can conclude that the contrast of the objects observed by a vision system with a wide directional pattern under field conditions was characterized by a steadily decreasing behavior. The contrast of the under-object (shadow) zone depends on the object's reflection coefficient. The image contrast of the objects observed by a vision system with a narrow directional pattern (under laboratory conditions) has a nonmonotonic behavior. It increased with the decrease of the object's size for systems with the narrow directional pattern. The contrast was maximum at the depth of about 0.8 of the limiting visibility depth. The growth and drop-down rates depended on the medium transparency. For objects with high reflection coefficient, the useful signal and the contrast increased near the level of objects invisibility with the decrease of the thickness of the gated medium layer.

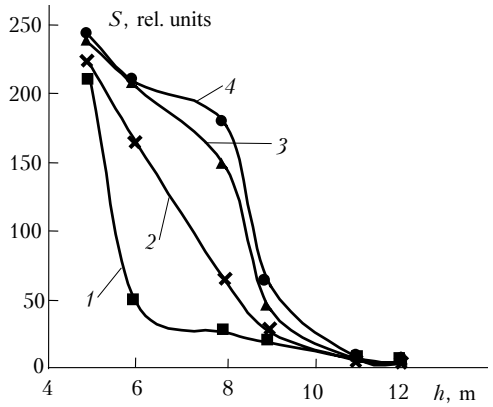

Fig. 5*a*. Depth dependence of the useful signal S for objects with different reflection coefficients R (dimensions of all objects 100 × 80 mm, water transparency by the Secchi disc ~ 11 m): R ~ 0.02 (curve *1*), ~ 0.05 (*2*), ~ 0.2 (*3*), ~ 0.25 (*4*).

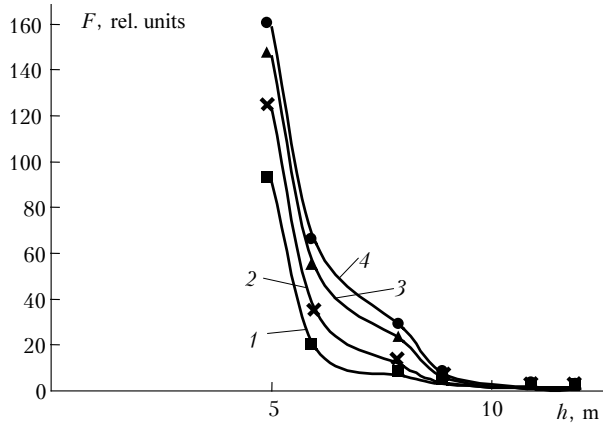

Fig. 5*b*. Depth dependence of the background F created by the image for objects with different reflection coefficients R (dimensions of all objects 100 × 80 mm, water transparency by the Secchi disc ~ 11 m): R ~ 0.02 (curve *1*), ~ 0.05 (*2*), ~ 0.2 (*3*), ~ 0.25 (*4*).

References

1. R.M. Measures, *Laser Remote Sensing, Fundamentals and Applications* (Wiley Interscience, New York, 1984).
2. K.Ya. Kondratyev and R.V. Pozdnyakov, *Optical Properties of Natural Waters and Remote Sensing of Phytoplankton* (Nauka, Leningrad, 1988), 181 pp.
3. V.M. Avetisyan et al., Issled. Zemli iz Kosmosa, No. 3, 81–86 (1988).
4. V.L. Veber and L.S. Dolin, Atmos. Oceanic Opt. **12**, No. 4, 285–290 (1999).
5. L.S. Dolin and I.M. Levin, *Reference Book on Underwater Vision Theory* (Gidrometeoizdat, Leningrad, 1991), 229 pp.
6. http://www.bifo.ru